Technical Report
University Of Wisconsin-Madison

(To be completed by RSP or the Department)

Project Title:	**Clouds of Uranus and Neptune**
Award Number:	**NNX09AB67G**
UW Account Number:	**PRJ23WQ**
For the Period of:	**1/1/2010 through 12/31/2010**
Principal Investigator:	**Lawrence Sromovsky**
Date Submitted:	**12/07/2010**
Location:	**University of Wisconsin Madison Space Science and Engineering Center 1225 West Dayton Street Madison, WI 53706**
Reports will be sent to:	**Philippe Crane philippe.crane@nasa.gov NSSC-Grant-Report@mail.nasa.gov**
SSEC Number (Internal)	***6457*** **I:/jennyh/Reports/6457Year2-NNX09AB67G.doc**

(To be completed by the Principal Investigator)

Inventions Report:

☒ No Inventions resulted from this award
☐ Yes

Inventory Report:

☒ No federally owned equipment is in the custody of the PI
☐ Yes

Publications: (Please list)

Fry, P.M. and L. A. Sromovsky, Implications of New Methane Absorption Coefficients on Uranus Vertical Structure Derived from Near-IR Spectra 2009. Bull. Am. Astron. Soc. 41, p 1010.

Kim, J. H., L. A. Sromovsky, and P. M. Fry, Radiative Transfer Modeling on the Atmosphere of Uranus. 2010. Bull. Am. Astron. Soc. 41, p 1022. (Supported mainly by a grant from the Space Telescope Science Institute.)

Kim, J.H., L. A. Sromovsky, and P. M. Fry, The distribution of cloud particles in the atmosphere of Uranus as constrained by STIS observations with Raman scattering and polarization effects included. In preparation for submission to Icarus.

Summary of Technical Effort:

OBJECTIVES: Our main objectives are to determine what the clouds of Uranus and Neptune are composed of, what their parent gases are, how they respond to seasonal forcing, how cloud bands differ from discrete features, and what their short-term and long-term variations are. The high-quality observations to be used to further these aims are Hubble Space Telescope observations at visible and near-IR wavelengths and intensive ground-based observations of Uranus at near-IR wavelengths. More recent observations include NICMOS observations made in 1997, as well as Cycle 17 observations both General Observer (Sromovsky PI) and Snap (Rages PI) programs, although the initial analysis of Cycle 17 observations will be funded by STScI grants.

RESULTS FROM YEAR TWO:

Increased Staffing: Last year we got behind in our analysis efforts because of inadequate staffing to meet all our commitments, and a time consuming search for a suitable postdoc candidate. In April 2010, our manpower problems were eased by the hiring of Dr. Joo Hyeon Kim as a postdoctoral associate in planetary atmospheres. Dr. Kim comes to us from JPL, where he had a NASA postdoctoral fellowship supervised by Kevin Baines. He is familiar with spectral analysis, having worked on the analysis of VIMS observations of Saturn. He has been learning how to use our software while he began efforts to model STIS observations of Uranus.

Software: We adapted our Levenberg-Marquardt fitting code to operate with both the near-IR and CCD spectral range radiation transfer calculators. The near-IR calculator makes use of parallel processors to simultaneously evaluate each of the 10 terms of the

exponential sums needed for modeling methane absorption at near-IR wavelengths. The CCD range calculator includes Raman scattering and either approximate or rigorous polarization calculations. We also developed extraction software to simultaneously obtain center-to-limb profiles from multiple band pass images (for HST ACS and WFPC2 images) and from spectral data cubes (in the case of STIS observations). We followed the Karkoschka & Tomasko (2009, Icarus 202, 287-309) approach of fitting the CTL profiles so that they could be sampled at the same viewing geometries at all latitudes, which in some cases requires small extrapolations to view angles that not directly observable. For the STIS 2002 observations the difference between solar and observer zenith angles can be ignored because the phase angle is very close to zero. This is not the case for many of the other observations, where the phase angle can reach several degrees. For those we fit I/F as a function of the $\mu\mu_o$ product (where μ and μ_o are the observer and solar zenith angles respectively), and then evaluate the functions for $\mu=\mu_o$, removing the first-order effect of the small phase angle. A sample extraction from HST ACS images is shown in the adjacent figure, where bright curved lines on the images indicate the sampled latitude, and the I/F values at each of eight different observer (and solar) cosines for each of the 15 images are plotted in comparison with a disk-integrated spectrum at the bottom.

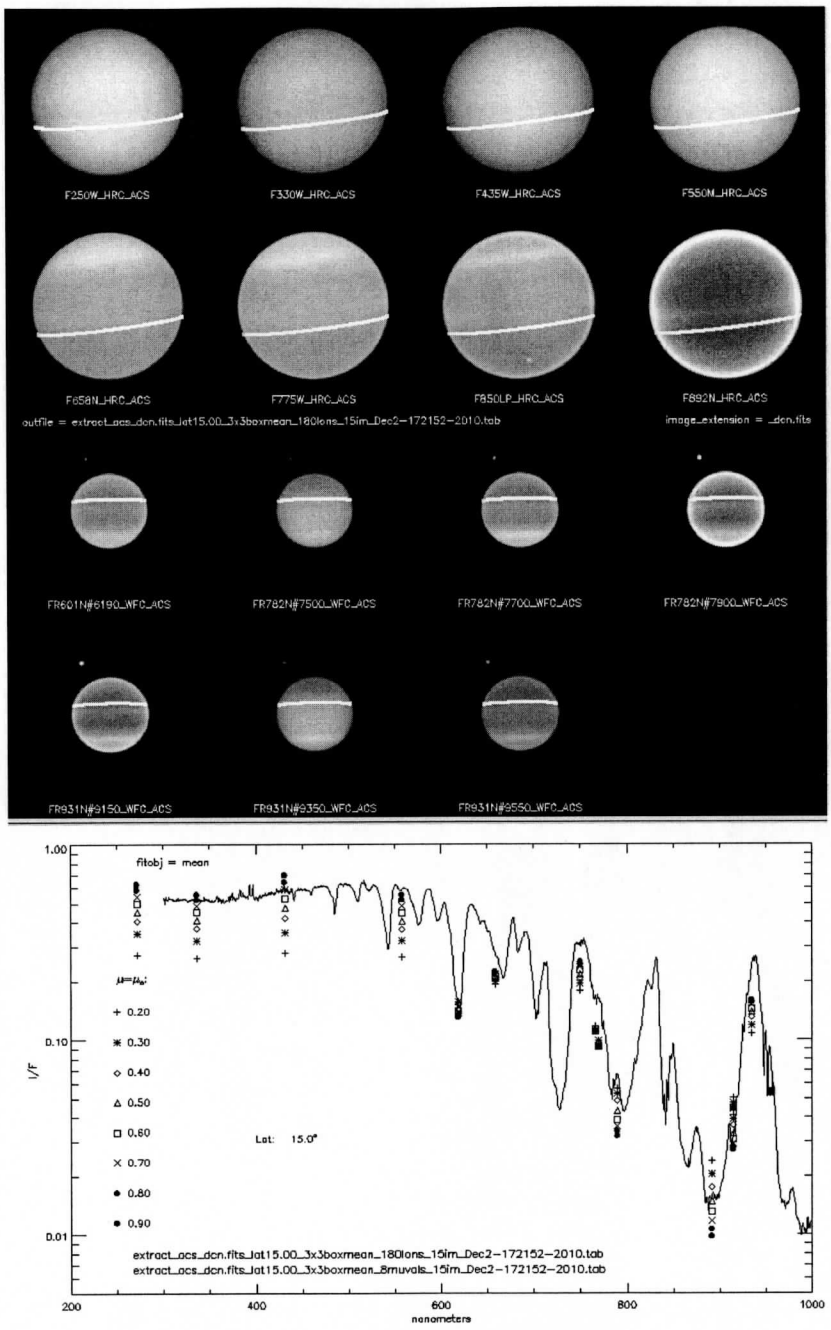

Modeling results. We began with modeling of STIS observations, which provides spatially resolved spectra over half of the Uranus disk during 2002. These

observations were well fit by Karkoschka and Tomasko (Icarus 202, 287-309, 2009) but are worth reanalysis for several reasons: (1) we can include accurate Raman scattering, which was only roughly approximated in the prior analysis, (2) the degree to which parameters of the model are constrained by the observations is not well defined and thus uniqueness is a serious issue and other models are likely possible, (3) the assumed wavelength dependence of the phase function is non-physical in the sense that most particles produce increased backscatter with increasing wavelength rather than the opposite, which is the characteristic of the K-T model, making it worthwhile to test other solution with more plausible physical characteristics, (3) recent analysis of IR spectral observations by Irwin et al. (2010, Icarus 208, 913-926) suggest a compact cloud layer with pressure increasing towards the equator instead of the vertically diffuse layers and latitude-independent vertical boundaries of the K-T model, (4) the vertical scale is highly dependent on the temperature profile and assumed methane humidity structure, which is not well established by the prior analysis, and (5) the key evidence for variations in methane mixing ratio with latitude did not account for the way pressure variations would affect the CH_4/H_2-He absorption ratio. Also the rejection of the compact cloud layer models stated in the K-T paper, did not make use of optimization of such models to fit the observed spectra, but rather on general characteristics. While the Karkoschka model provides a good fit to the observations, it is far from clear how well that model is constrained, and to what degree other models could also fit the observations. To assess the quality of the K-T model we implemented that model in our software and allowed the optical depths per bar of each of the four layers to be

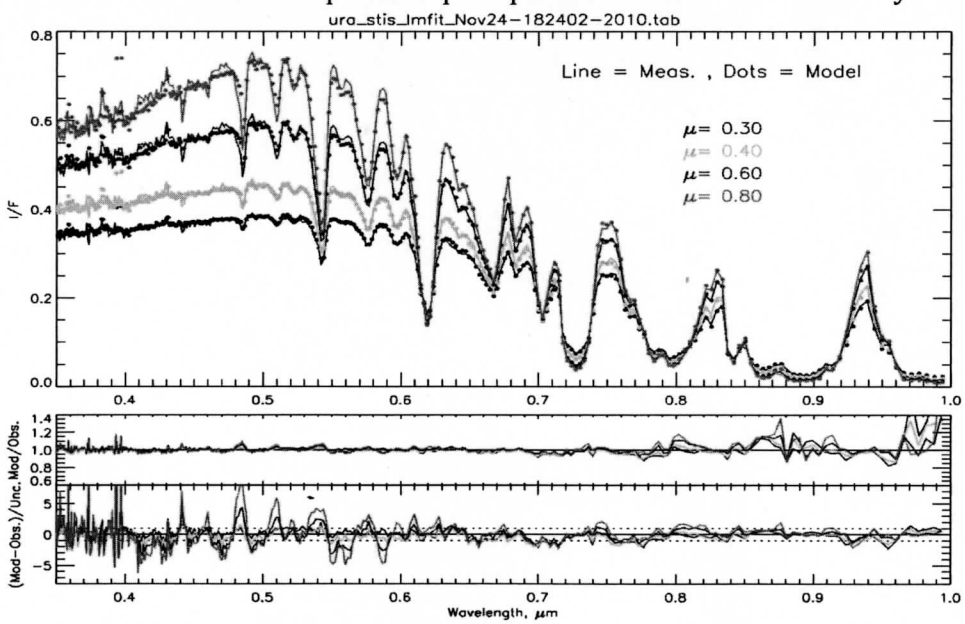

adjusted by the fitting algorithm. A sample fit is shown for four view-angle cosines (0.3, 0.4, 0.6, and 0.8) at latitude 45° S, where Uranus bright band is observed. This fit includes Raman scattering. The largest absolute uncertainties are at the longer wavelengths in the deep methane bands, while the largest errors relative to expected uncertainties are at shorter wavelengths, where weak methane bands and Raman features are not well fit for two likely reasons: (1) the weak methane bands

were derived from a procedure that incorrectly corrects for Raman scattering effects, as pointed out by Sromovsky (Icarus 173, 245-283, 2005), and (2) the vertical distribution of aerosols does not have sufficient opacity at high altitudes, which is needed to damp the Raman scattering features.

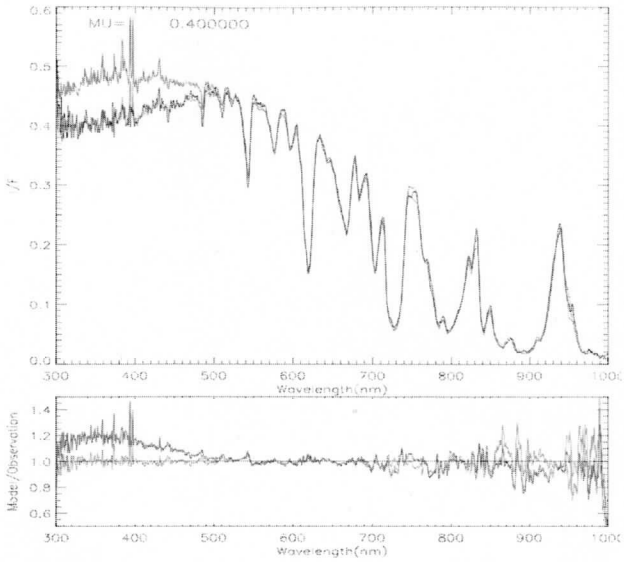

The simpler models we started exploring for modeling the STIS observations were constructed of two Mie particle layers, with adjustable particle size, pressure, and optical depth; we started by assuming a real imaginary index and restricted our fits to wavelengths beyond 550-600 nm to avoid the region where significant absorption must be included. The fit at right (blue curve) was constrained only by the observations from 600 to 860 nm. Our plan was to constrain, using this range, the particle size, number density, and vertical location, and then to adjust the imaginary index at short wavelengths as needed to fit the observations. This simpler model of two compact layers produces the blue spectrum in the above figure, while the much more complex 4-layer K-T model is shown in red, with the observations in black. The simpler model yields a fit comparable to the more complex model for wavelengths greater than 500 nm, and presumably will also be comparable at shorter wavelengths once we add absorption to the upper layer of Mie particles. These two Mie layers have particle sizes 0.06 and 0.2 microns, optical depths of 0.1 and 5.5, and pressures of 1.2 and 2.2 bars, respectively. The addition of an upper level haze, or making the upper cloud more vertically extended, will likely be needed to match the Raman features near 400 nm. Preliminary work on these models, which was supported mainly by a grant from the Space Telescope Science Institute, was reported by Dr. Kim at the last DPS meeting in Pasadena in early October 2010.

We have also been fitting models to band-pass filter images, as part of the preliminary analysis supported by STScI grants. To simplify the analysis of these images we reduced the number of free parameters to four, just the optical depths of the four layers of the K-T model, which is otherwise used to constrain all the other particle properties. The preliminary results are shown in the following figure for two different data sets: (1) 2006 ACS imaging observations, as shown in the first figure in this report, and (2) 2007 WFPC2 images obtained through a Snap program (K. Rages PI). (Note that the figure legend refers to observation dates rather than publication dates.) These fits are shown with three vertical lines: the best-fit value with lower and higher limits. The ACS results (dotted lines) are the best constrained because of the larger number of well-placed filters. The WFPC2 fits (dot-dash) are much more uncertain. The K-T results are shown as solid vertical bars, while the

recent Irwin et al results are shown as dashed curves. These are all in crude agreement, but have some notable differences. The best-constrained parameter is the middle tropospheric cloud (1.2-2 bars), but the fits of Irwin et al, based on near-IR spectra, yield a peak cloud density that is deeper than assumed for the K-T (Karkoshka-Tomasko) model. This is likely due to the different vertical profiles of methane assumed in the different models. The Irwin et al. results shown are for a 30% relative methane humidity above the 1 bar level, the Lindal D T-P profile, and a 1.6% methane volume mixing ratio, while K-T used a higher methane humidity

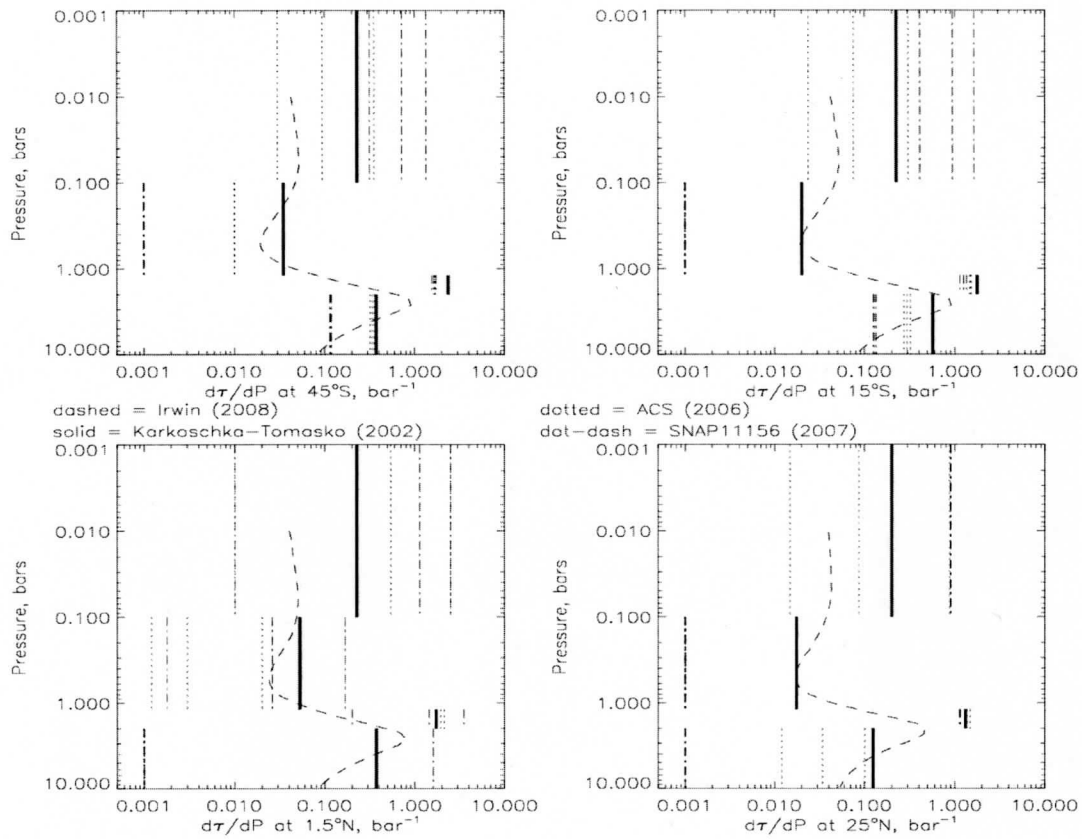

(with a temperature profile even warmer than the Lindal F solution) just above the 1.2-bar level, but decreasing with altitude. The K-T methane amount is greater at lower pressures, and thus cloud particles must be at lower pressures to produce the observed I/F. It is interesting that our 2 Mie-layer model of the STIS spectrum has its most opaque compact layer near the bottom of the K-T middle tropospheric cloud and close to the peak of the distribution obtained by Irwin et al. (2009). We will next try to fit the HST band pass filter images using such a model.

The near-IR analysis has been proceeding more slowly, due to difficulty obtaining accurate fits to the observations. The target of the fits initially has been the 2006 NIRC2 Keck II observations of central meridian spectra in J and H bands. Our initial fits to these data using reflecting layer models compared results using two different absorption models: Irwin (Icarus, 2006) and Karkoschka (2009). The results (Fry and Sromovsky 2009) indicated that the Karkoschka 2009 coefficients made a substantial improvement to the fit quality in the J band but relatively little

difference in the H band. Irwin et al. (2010) found that the new Karkoschka coefficients greatly improved the consistency between retrievals from the two separate bands. A sample of one of our fits to our NIRC2 spectrum at 12° S is provided in the following figure. Here solid lines indicate measurements and dotted lines indicate uncertainty limits. The filled circles show the model calculations.

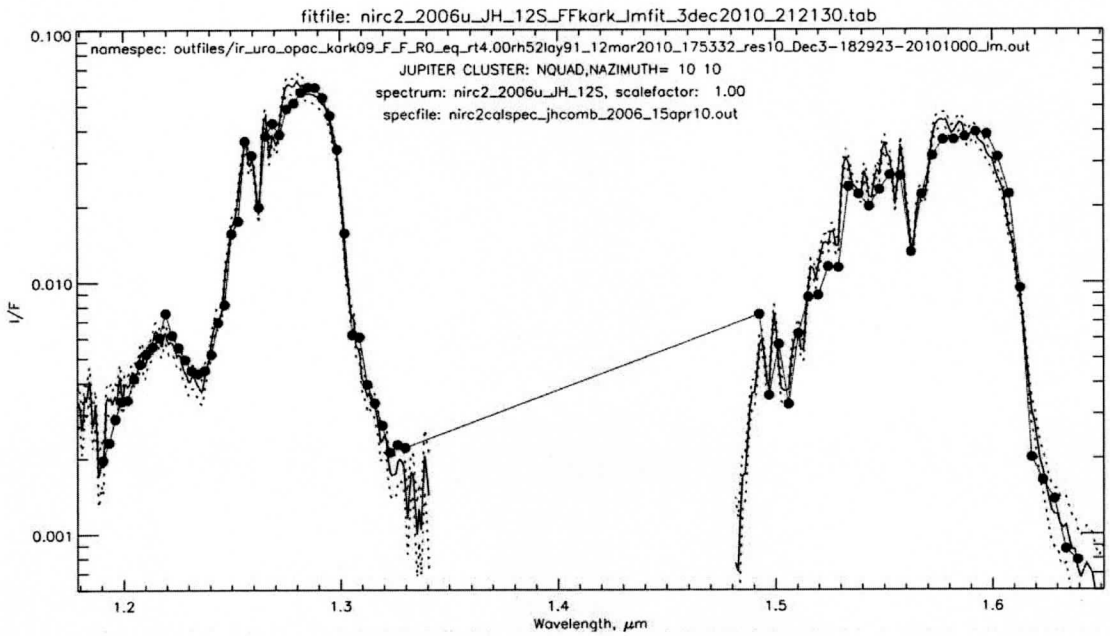

This solution is for the Lindal (JGR 92, 14987-15001,1987) model F, which had a 4% deep methane mixing ratio and a relatively high above-cloud methane humidity. The cloud structure model we used for this particular fit consisted of two compact Mie layers, with real index of 1.4. The adjustable parameters were the particle radii, the two layer pressures, and the optical depths. The best-fit values were 0.57 bars and 1.69 bars for the pressures, 0.15 and 2.81 for the particle radii, and 0.001 and 0.45 for the optical depths, although all these parameters have significant uncertainties. The pressure of the main cloud is similar to pressures obtained from the 2-layer Mie particle fit to the STIS spectra, although the particle radius is much larger for the bottom layer. The optical depth for the bottom layer is much smaller for this near-IR fit (referenced to 2 microns) than it is for the 0.5 micron referenced STIS fit (by a factor of 10), which might be a result of a large wavelength dependence in scattering efficiency, indicative of particles smaller than the best fit values obtained from the near-IR analysis. It will be our objective to find physically consistent solutions that apply to both near-IR and CCD spectral ranges. We are not yet very close to that ideal.

The vertical and latitudinal distribution of methane on Uranus. There are two features that have important effects on the observed spectrum of Uranus. One is the "above cloud" mixing ratio profile, and the other is the "deep" mixing ratio. There is a considerable range available from the set of solutions Lindal et al. (1987) derived to match the observed refractivity profile at the latitude of the occultation (2-7° S). These range from A (no methane) to F (4% deep methane), and only D, E, and F have any

methane at all above the nominal cloud top. The cloud inferred from refractivity was centered at 1.2 bars and had a scale height of 2-4 km. Previously, we attempted to determine the methane mixing ratio by finding which of the Lindal solutions allowed cloud models to provide the best match to the observed spectrum. This made sense at low latitudes near those in which the occultation was measured, but was not appropriate at other latitudes because variations in methane mixing ratio would be accompanied by temperature structure variations that would imply large vertical wind shears, as well as violating observed constraints on latitudinal variations in temperature. Karkoschka and Tomasko (2009) assumed that the T(P) profile was invariant with latitude, but allowed the methane mixing ratio of the deep atmosphere to vary, which creates density variations with latitude that also lead to vertical wind shears (Sun et al., Icarus 91, 154-160, 1991). If these density gradients extend to great depths the resulting implied wind fields would be in conflict with observations; thus the latitudinal gradients in methane, if present, cannot extend to great depths.

The variation with latitude inferred by Karkoschka and Tomasko (2009) is based on different latitudinal I/F profiles of wavelengths with different amounts of methane and CIA absorption contributions. A variation in latitude of the I/F at a methane dominated wavelength (blue curve at right) could be due to clouds variations or variations in methane; but a lack of variation in the I/F at a wavelength with similar absorption, but dominated by CIA (red curve above) suggests that it the clouds are not varying with latitude, implying that methane does vary.

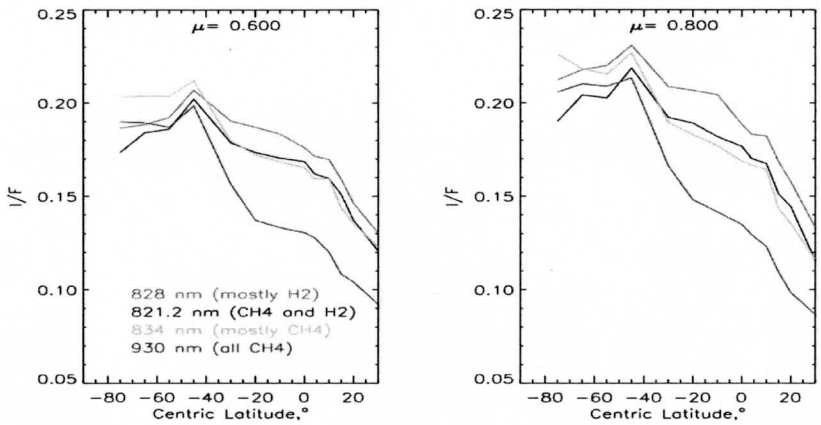

However, CIA and methane absorption have very different vertical variations, as shown in the example plotted at the right. This shows that four wavelengths with nearly identical transmissions to the 1.5-bar level can have very different transmissions to other pressure levels. The H2-CIA curve (red) shows lower transmission than methane (blue) at low pressures, but higher transmission at higher pressures. The ratio of all curves to the CIA curve is shown in the bottom panel. From this it is conceivable that a change in cloud pressure with latitude might lead to a variation in I/F at methane-dominated wavelengths that is not as prominent at CIA wavelengths of similar absorption. In fact, a

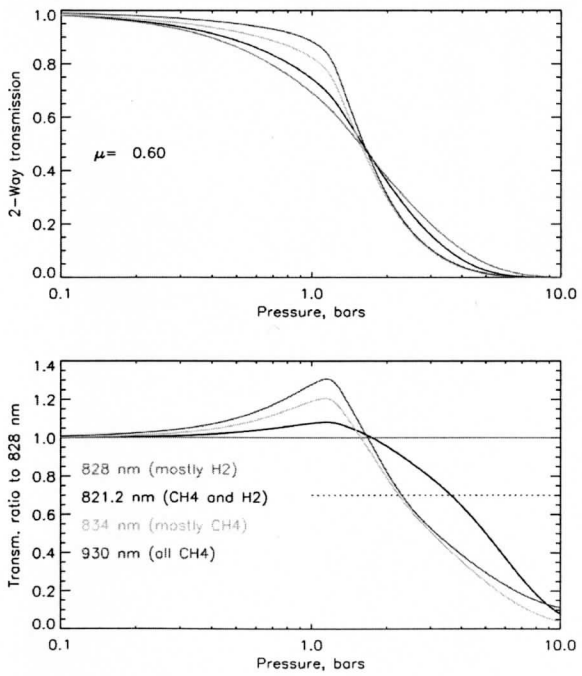

deeper cloud near the equator is inferred from Irwin et al. (2006). This issue needs further investigation.

From the stratosphere to the cloud level, Karkoschka and Tomasko (2009) assumed a methane profile that did not vary with latitude, primarily based on the relatively flat latitudinal profile seen in the strongest methane bands, and adopted a methane mixing ratio profile that had humidity decreasing with altitude, using the functional form $RH=48\%[1-(1-P)^2]$, where P is the pressure in bars, but used only for P<1.15 bars. They claimed that a constant humidity profile would require more aerosol opacity between 0 and 0.5 bar than between 0.5 and 1 bar, which they deemed to be unphysical based on the haze modeling work of Rages et al. (1991, Icarus 89, 359-376). However, this does not seem to be a compelling argument because some component of the haze could evaporate at the warmer temperatures present at the higher pressures. In fact there solution, even for the decreasing humidity case, does have a total opacity above the 0.1 bar level comparable to that between 0.1 and 0.9 bar; which is also a violation of the Rages et al. model. Perhaps a better argument for a decreasing humidity profile is that the low stratospheric mixing ratio is compatible with a very low humidity at the tropopause level (about 12%).

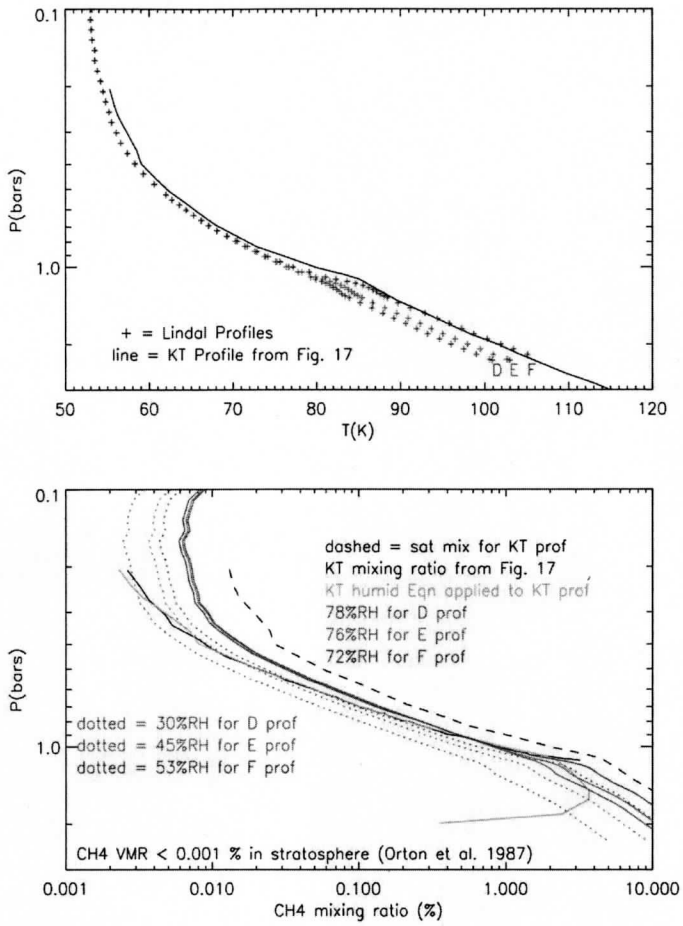

Another factor that increased the methane mixing ratio for a given assumed humidity is that K-T did not use any of the Lindal et al. temperature profile solutions, but chose one even warmer than the warmest F profile, which is presumably due to inclusion of a mixing ratio of 0.0004 of Neon in the atmosphere (Karkoshka, personal communication). Karkoshka thought that this only made a difference of 0.4 K in the temperature profile, but the digitized plot in the above figure indicates a much larger difference (up to ten times more in the 1-1.21 bar region). To match their mixing ratio profile, using the model F T-P profile, we used a function of the form $RH = RH_{max}$ $(RH_{min}/RH_{max})^{\wedge} [(1-P_{max}/P)/(1-P_{max}/P_{min})]$ separately applied over two regions: for 0.1 bar < P < 1 bar, we used $RH_{min}=12\%$ and $RH_{max}=65\%$; and for 1 bar < P < 1.13 bars, we used $RH_{min}=65\%$ and $RH_{max}=76\%$. This yields a methane mixing ratio at the troposphere of 1E-5, which is in agreement with the stratospheric value of Orton et al. (1987, Icarus 70, 1-12), but leads to notably greater methane mixing ratios near 1 bar than even Lindal's model F solution. This issue also needs to be reviewed.

We also tested calibration consistency between STIS and the HST band pass imaging observations of Uranus. At a given latitude, I/F ratios varied significantly with view angle, unless the HST imaging was deconvolved, in which case consistency was good up to mu=0.4, but there was a slight trend for ACS to become dimmer than STIS at larger view angles (smaller mu values). For mu=0.6, we show in the following figure the ACS(deconvolved) / STIS I/F ratio vs. wavelength for latitudes from 44S to 20 N.

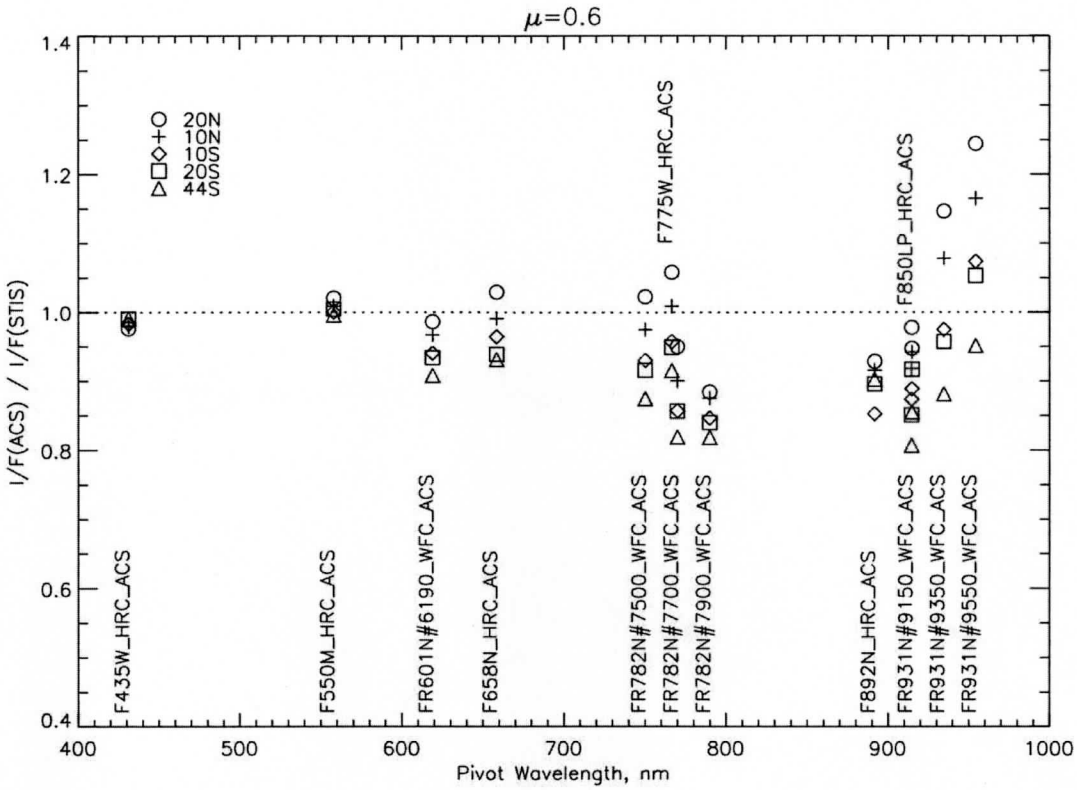

This suggests a possible calibration discrepancy at longer wavelengths, although part of this variation could be due to temporal changes. Another useful comparison at the long wavelength (0.83-1.0 micron) part of the spectrum is with IRTF spectra obtained in 2006 (Sromovsky and Fry, Icarus 193, 252-266). This will be carried out during the coming year. We will also make similar comparisons with WFPC2 and WFC3 observations in 2007 and 2008.

PLANS FOR NEXT YEAR:

We will review the issues of vertical distribution of methane, appropriate temperature structure consistent with occultation results, and the implications of mixing ratio variations on vertical wind shears and vertically integrated wind differences as a function of the depth to which methane mixing ratio variations are extended. This may result in a paper describing constraints on the suggested variations.

We will also review the calibration consistency of the STIS cube, ACS, and WFPC2 and WFC3 band pass filter images, and IRTF spectra and identify any potential impacts on

the interpretation of secular variations. The disk-integrated I/F results from HST observations will be compared with the recent record of ground based observations of Lockwood at Lowell Observatory, with the aim of illuminating how changes in Uranus cloud structure lead to the observed secular variations.

The main focus will be on assessing different kinds of cloud models that can be used to fit the STIS spectra of Uranus. This will form the basis of a paper to be submitted to Icarus. A second paper will be prepared to assess the types of models than can be used to explain the band pass filter images of Uranus obtained from HST WFPC2, ACS, and WFC3, also aimed for submission to Icarus. The changes in cloud structure over time will be a significant topic in that investigation.

A third paper will be prepared to assess the kinds of particle distributions that can fit the near-IR spectra of Uranus, including Keck NIRC2 grism spectra, and NICMOS and WF3 observations from HST. A unifying aim of all these papers will be to try to find distributions and particle compositions that can fit both CCD and near-IR spectral ranges. We will also turn our attention to secular variations of both Uranus and Neptune, using the HST images acquired over the last decade to determine the disk-integrated brightness over time and relate that to the long-term ground based observations and to the distribution and character of cloud bands and discrete features on both planets. We will also focus on the differences in vertical cloud structure between Uranus and Neptune, based on WFPC2 and near-IR observations.